ISSN 0020-1685, Inorganic Materials, 2015, Vol. 51, No. 12, pp. 1288–1295. © Pleiades Publishing, Ltd., 2015.
Original Russian Text © A.M. Kut'in, A.D. Plekhovich, A.A. Sibirkin, 2015, published in Neorganicheskie Materialy, 2015, Vol. 51, No. 12, pp. 1385–1392.

Crystallization Kinetics of $(TeO_2)_{1-x}(MoO_3)_x$ Glasses Studied by Differential Scanning Calorimetry

A. M. Kut'in[a, b], A. D. Plekhovich[b], and A. A. Sibirkin[a]

[a] *Lobachevsky State University, pr. Gagarina 23, Nizhny Novgorod, 603950 Russia*

[b] *Devyatykh Institute of Chemistry of High-Purity Substances, Russian Academy of Sciences, ul. Tropinina 49, Nizhny Novgorod, 603950 Russia*

e-mail: plehovich@gmail.com

Received May 18, 2015

Abstract—A technique has been proposed for assessing kinetic characteristics (parameters) of glass crystallization from mathematical data processing results for glass crystallization peaks, with allowance for nonisothermal conditions of differential scanning calorimetry. The technique has been used to analyze the crystallization behavior of $(TeO_2)_{1-x}(MoO_3)_x$ ($x = 0.25$–0.55) glasses, which has made it possible to evaluate crystallization parameters and derive their regression dependences on glass composition. Basic to glassy materials research is that the proposed approach includes a parametrically defined, explicit functional dependence of the degree of crystallization on time and temperature, $\alpha(t, T)$, as a basis for optimizing glass heat treatment conditions in terms of this characteristic and predicting such conditions from regression relationships for previously unexplored compositions in the tellurite–molybdate glass system studied.

DOI: 10.1134/S0020168515120055

INTRODUCTION

Tellurite–molybdate glasses prepared from precipitates obtained by adding aqueous ammonia to hydrochloric acid solutions of tellurium(IV) and molybdenum(VI) compounds offer low optical absorption in the visible and near-IR spectral regions [1–3] and are thus promising materials for fiber-optic applications. Glass transition temperatures determined by differential scanning calorimetry (DSC) for samples of various compositions were reported to be close to those of glasses prepared by melting oxide mixtures [4].

One possible reason for additional optical losses in glass is the formation of crystalline inclusions as a consequence of nonoptimal melt cooling and glass heat treatment schedules. Glass crystallization kinetics in the system in question has not yet been studied.

Thermal analysis techniques are being used increasingly in studies of glass crystallization [5, 6]. The reason for this is that these techniques provide clear, informative data on the crystallization behavior of glasses in the form of corresponding peaks, ensure high-speed measurements, and employ advanced, readily available DSC instruments. Unfortunately, existing techniques for mathematical processing of crystallization peaks [7, 8] as a rule do not fully take into account that DSC measurements are made under nonisothermal conditions. An even more serious drawback of these techniques is that the dependence of model exponents on the heating rate is not substantiated physically.

The objectives of this work were

to choose and improve a procedure for DSC data processing using test data on the crystallization kinetics of glassy GeS_2 and

to find kinetic characteristics of crystallization by processing DSC data for a series of $(TeO_2)_{1-x}(MoO_3)_x$ glasses and determine the degree of crystallization as a function of temperature and time with the aim of minimizing the crystallization effect in optical applications of tellurite–molybdate glasses.

MATHEMATICAL MODEL FOR PROCESSING DSC PEAKS OF CRYSTALLIZATION

The enthalpy increment ΔH for the crystallization of glass A, represented by the quasi-chemical reaction $A \rightarrow {}^*A$, is determined [9] by a molar coordinate ξ and the enthalpy of the crystallization reaction $\Delta_r H$:

$$\Delta H = \xi \Delta_r H = \alpha n_0 \Delta_r H = \alpha m_0 (\Delta_r H / M). \quad (1)$$

The second and third expressions in (1) include the degree of crystallization, $\alpha = \xi / n_0$, as the fraction of the number of moles, ξ, relative to the initial amount, $n_0 = m_0 / M$, of the starting (mother) phase (where m_0 and M are, respectively, the initial and molar masses of the crystallizing substance).

Dividing Eq. (1) by m_0, we obtain a relation between the enthalpies under consideration and, accordingly, between the corresponding heats in specific quantities, that is, per unit mass:

$$\frac{\Delta H}{m_0} = \alpha\frac{\Delta_r H}{M}, \quad Q_m = \alpha Q_{rM}. \qquad (1')$$

The second equation in (1') relates the specific heat $Q_m = -\Delta H/m_0$ to the specific heat of the reaction: $Q_{rM} = -\Delta_r H/M$.

Within certain limits, a signal proportional to the specific heat flux, $\dot{Q}_m = dQ_m/dt$, in heat-flow DSC instruments is commonly believed to be independent of the mass of the sample [10]:

$$S_{DSC} = C\dot{Q}_m = C\dot{\alpha}Q_{rM} = C_N\dot{\alpha}, \qquad (2)$$

where the flux $\dot{Q}_m = \dot{\alpha}Q_{rM}$ is obtained by differentiating the second equation in (1') with respect to time. Thus, at constant C and Q_{rM}, the shape of the crystallization peak is determined by the crystallization rate $\dot{\alpha} = d\alpha/dt$, and its area is determined by the integral of relation (2), which is $C\alpha Q_{rM}$. Clearly, the area of the entire peak after the crystallization of the sample ($\alpha = 1$) is CQ_{rM}.

Such reasoning is applicable as well to melting peaks, which are used to calibrate instruments. Therefore, the magnitude and dimensions of the instrumental or normalization constant $C_N = CQ_{rM}$ for a calibrated instrument ($C = 1$) correspond to those of the specific heat of the process, Q_{rM} (J/g), ensuring the dimensions of the DSC signal (J/(g s)) as a specific heat flux or specific power.

When the dimensions of the S_{DSC} signal of an uncalibrated instrument are μV/mg, the dimensions of the normalization constant are $[C_N] = [S_{DSC}/\dot{\alpha}] = \mu V\ s/mg$.

The Johnson–Mehl–Avrami (JMA) model, which is most frequently used to determine the crystallization rate $\dot{\alpha}$, is a considerable simplification of the Kolmogorov–Johnson–Mehl theory. In this three-parameter model, the degree of crystallization as a function of temperature and time has the form

$$\alpha(t, T) = 1 - \exp(-\tau^n), \qquad (3)$$

where $\tau = kt$; $k = A\exp(-E_a/(RT))$ is the crystallization rate constant in Arrhenius representation; A is the preexponential factor; E_a is the activation energy; and n is the JMA exponent, which qualitatively corresponds to the size parameter in the Kolmogorov–Johnson–Mehl theory. To the integral form of the JMA model (3) corresponds its differential form:

$$\dot{\alpha} = \frac{d\alpha}{dt} = k\alpha'_\tau(\alpha); \quad \alpha'_\tau(\alpha) = n(1-\alpha)[-\ln(1-\alpha)]^{1-1/n}. \qquad (4)$$

Note that the derivative of α with respect to dimensionless time τ is denoted in the literature by $\alpha'_\tau(\alpha) = f(\alpha)$.

Another simplified, semiempirical form of the Kolmogorov–Johnson–Mehl theory was proposed by Erofeev [11]. The differential equation representing this semiempirical model has the form

$$\dot{\alpha} = k_{eff}\alpha^a(1-\alpha)^b. \qquad (5)$$

As shown by Sestaik and Berggren [12] and then by Malek et al. [7], the semiempirical model has an advantage over the JMA model in processing DSC peaks due to crystallization. At the same time, the lack of an analytical solution to the differential equation for the semiempirical model or its integral form $\alpha(t, T)$ complicates numerical processing of experimental data, makes it difficult to fully take into account that DSC measurements are made under nonisothermal conditions, and markedly limits the model's predictive power, which is quantified by a parametrically defined, explicit function: $\alpha(t, T)$. Another important drawback to the semiempirical model is that its meaning is hidden in the empirical exponents a and b and that the rate constant k_{eff} has an effective character. These factors make it difficult to identify details of the crystallization mechanism in terms of the Kolmogorov–Johnson–Mehl concepts.

A modified semiempirical (MSE) model we propose here is free of the above drawbacks. Its integral form is represented by

$$\alpha(t, T) = \frac{1}{(1 + 1/\tau^n)^p}. \qquad (6)$$

Comparison of formulas (3) and (6) suggests a procedure—common to the JMA and MSE models—for determining the temperature–time dependence $\alpha(t, T)$ only through the $\tau = kt$ product.

Differentiating relation (6) yields an appropriate differential form of the MSE model:

$$\dot{\alpha} = \alpha'_\tau\tau'_t = k\alpha'_\tau = knp\alpha^{1-1/(np)}(1-\alpha^{1/p})^{1+1/n}. \qquad (7)$$

Comparison of formulas (4) and (7) indicates that the np product in the MSE model plays the role of the crystallization parameter n, which is important for the JMA model and effectively determines the crystallization mechanism. Finally, comparison of formulas (5) and (7) indicates that the MSE model discloses not only the meaning of the exponents a and b in the semiempirical model but also that of the effective rate constant k_{eff}.

Equation (4) for the JMA model and Eq. (7) for the MSE model correspond to isothermal kinetics because, when differentiating, the temperature-dependent rate constant k was taken to be time-independent. However, when thermal analysis is carried

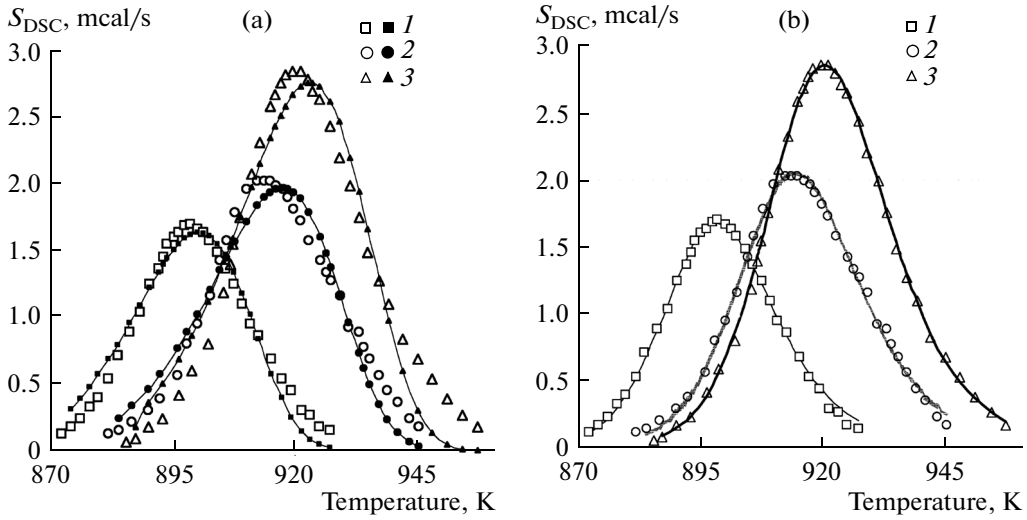

Fig. 1. Crystallization peaks of glassy GeS_2 at heating rates of (*1*) 5, (*2*) 15, and (*3*) 20 K/min [8] and calculation results: (a) JMA model (lines with appropriate filled data points), (b) MSE model (lines) with model parameters found by NR (see Table 1).

out at a constant heating rate (β), the temperature of the measuring cell in the problem under consideration, which is measured from the crystallization onset temperature T_0, is a linear function of time:

$$T = T_0 + \beta t. \quad (8)$$

The differentiation result in formulas (4) and (7), with allowance for (8) at a single temperature–time dependence (through the $\tau = kt$ product) and an Arrhenius form of k,

$$\dot{\alpha} = \frac{d\alpha}{dt} = \alpha'_\tau \tau'_{tt} = \alpha'_\tau k\left(1 + \frac{(T - T_0)\theta}{T^2}\right), \quad (9)$$

differs from relations (4) and (7) only by the factor in parentheses. If this factor is included in a "nonisothermal" rate constant in a natural way,

$$\bar{k} = k\left(1 + \frac{(T - T_0)\theta}{T^2}\right), \quad (10)$$

and k is replaced by $\bar{k}$, (9) reproduces (4) and (7).

That the JMA and MSE models have an explicit expression for the degree of crystallization significantly simplifies the parameterization problem in processing DSC peaks due to crystallization, reducing it to nonlinear regression (NR) with standard procedures for minimizing the root mean square deviation between the measured SC signal and the values calculated using Eqs. (2)–(4), (6), (7), and (10). Comparison of data processing results for crystallization peaks of glassy GeS_2, which was used as a test system by Malek and Klikorka [8], in the JMA and MSE models in Fig. 1 clearly demonstrates the advantages of the latter model in studies of glass crystallization kinetics.

In interpreting the data processing results for the crystallization peaks of GeS_2 in a known model and in the model under development, with allowance for nonisothermal measurement conditions, it is worth noting that the so-called normalization constants C_{N_i} for the peaks corresponding to heating rates of 5, 15, and 20 K/min have an auxiliary character. They do not appear in the definition of the degree of crystallization, $\alpha(t, T)$, and depend, among other things, on the calibration of the instrument. The relatively poor description of the data in the JMA model is supplemented by the fact that the parameter $n = 1.061$ lies beyond the range 2–4, tolerable in the parent Kolmogorov–Johnson–Mehl theory. Note that the np product, which is used in the MSE model instead of this parameter is 2.468.

EXPERIMENTAL

The crystallization behavior of tellurite–molybdate glasses was studied using samples of five compositions: $(TeO_2)_{0.75}(MoO_3)_{0.25}$, $(TeO_2)_{0.65}(MoO_3)_{0.35}$, $(TeO_2)_{0.60}(MoO_3)_{0.40}$, $(TeO_2)_{0.55}(MoO_3)_{0.45}$, and $(TeO_2)_{0.45}(MoO_3)_{0.55}$. The glass preparation process and the impurity composition of the samples were reported previously [1–3, 13].

Measurements were performed with a Netzsch STA 409 PC Luxx simultaneous thermal analysis system at heating rates of 5, 10, 15, and 20 K/min and an argon flow rate of 34 mL/min.

For our experiments, we prepared a series of samples weighing 30–40 mg. The sample surface that was

Table 1. Model parameters evaluated by NR

Model	E_a, kJ/mol	A, s^{-1}	n	p	C_N, mcal		
					C_{N_1}	C_{N_2}	C_{N_3}
MSE	357.7	9.015×10^{17}	1.768	1.396	610.2	268.9	283.0
JMA	358.2	1.512×10^{18}	1.061		576.4	258.1	273.5

in contact with the crucible bottom was ground to ensure reproducible contact. Next, the samples were cleaned by ultrasonication in distilled water and dried. In our measurements, we used preannealed platinum crucibles, which are the least reactive with tellurite glasses.

Figure 2 presents DSC curves for three of the five samples studied. The curves were obtained at a constant heating rate of 15 K/min and show a region of a glassy state, a devitrification "step," a broad temperature range of a viscous flow state, and well-defined crystallization and melting peaks.

Table 2 summarizes data processing results for the DSC curves obtained at a heating rate of 10 K/min. The glass transition temperature was evaluated from the position of the inflection point in the DSC curve in the glass transition range, and the crystallization and melting points were determined from the peak onset temperature, that is, from the temperature at which the tangent to the ascending peak slope intersected the linearly extrapolated baseline.

It follows from Table 2 that the glass transition temperature T_g decreases with increasing molybdenum trioxide content. Note also that the melting points obtained by us for the different compositions are consistent with the phase diagram of the binary system TeO_2–MoO_3 [14].

For the purposes of this study, data analysis and processing were carried out in the crystallization region of the DSC curves.

Table 2. Glass transition temperature (t_g), crystallization temperature (t_x), and melting point (t_m) of the tellurite–molybdate glasses at a heating rate of 10 K/min

Composition	t_g, °C	t_{cr}, °C	t_m, °C
$(TeO_2)_{0.75}(MoO_3)_{0.25}$	318.1	460.2	527.4
$(TeO_2)_{0.65}(MoO_3)_{0.35}$	314.7	446.4	536.4
$(TeO_2)_{0.60}(MoO_3)_{0.40}$	311.7	450.1	516.0
$(TeO_2)_{0.55}(MoO_3)_{0.45}$	306.7	436.8	518.0
$(TeO_2)_{0.45}(MoO_3)_{0.55}$	303.9	441.3	522.0

RESULTS AND DISCUSSION

The experimental data and calculation results presented in Fig. 3 suggest that the MSE model offers good possibilities for describing crystallization in tellurite–molybdate glasses. At the same time, detailed analysis of crystallization peaks revealed features indicating that the glasses crystallized in two steps. The presence of additional crystallization peaks on top of the main peaks, which is the most pronounced for the glass compositions in Figs. 3d and 3e, can be accounted for in terms of the phase diagram (liquidus diagram) of the TeO_2–MoO_3 system [14]. In addition to phases determined by the end-members of the system (TeO_2 and MoO_3), the phase diagram reported by Petrini and Bart [14] shows the Te_2MoO_7 compound, which melts congruently at 551°C, and two low-temperature eutectics, containing 32.5 and 44.5 mol % MoO_3 and melting at 543 and 526°C, respectively. Thus, the additional peaks in Figs. 3c–3e are due to MoO_3 crystallization in parallel with the crystallization of the main phase Te_2MoO_7, and the shape of the

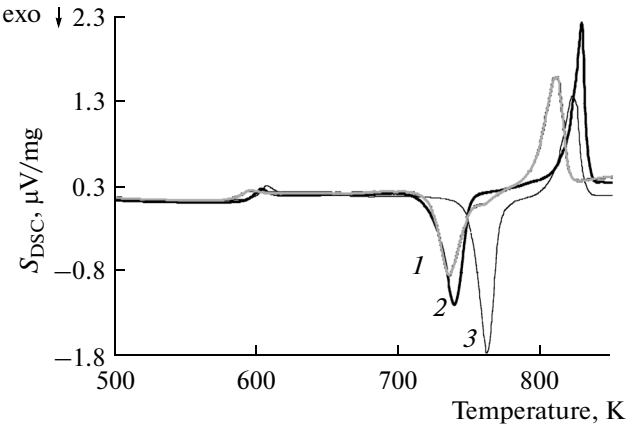

Fig. 2. DSC curves of tellurite glasses at a heating rate of 15 K/min: (*1*) $(TeO_2)_{0.55}(MoO_3)_{0.45}$, (*2*) $(TeO_2)_{0.65}(MoO_3)_{0.35}$, (*3*) $(TeO_2)_{0.75}(MoO_3)_{0.25}$.

Table 3. Kinetic parameters of the MSE model for the $(TeO_2)_{1-x}(MoO_3)_x$ ($x = 0.25$, 0.35, 0.40, 0.45, and 0.55) glasses

Composition	E_a, kJ/mol	s	n	p	np	C_N, μV s/mg		
						C_{N_1}	C_{N_2}	C_{N_3}
$(TeO_2)_{0.75}(MoO_3)_{0.25}$	120.9	13.08	6.89	0.579	3.99	110.2	88.57	84.38
$(TeO_2)_{0.65}(MoO_3)_{0.35}$	123.6	13.76	6.65	0.584	3.88	208.1	112.1	108.4
$(TeO_2)_{0.60}(MoO_3)_{0.40}$	120.5	13.78	4.84	0.770	3.73	115.0	83.07	87.43
$(TeO_2)_{0.55}(MoO_3)_{0.45}$	114.3	12.97	3.88	1.030	4.00	92.82	97.36	96.79
$(TeO_2)_{0.45}(MoO_3)_{0.55}$	97.51	10.55	3.87	0.842	3.26	79.09	93.37	84.19

E_a is the activation energy, $s = \ln(A/s^{-1})$ is the natural logarithm of the pre-exponential factor (s^{-1}), and n and p are exponents.

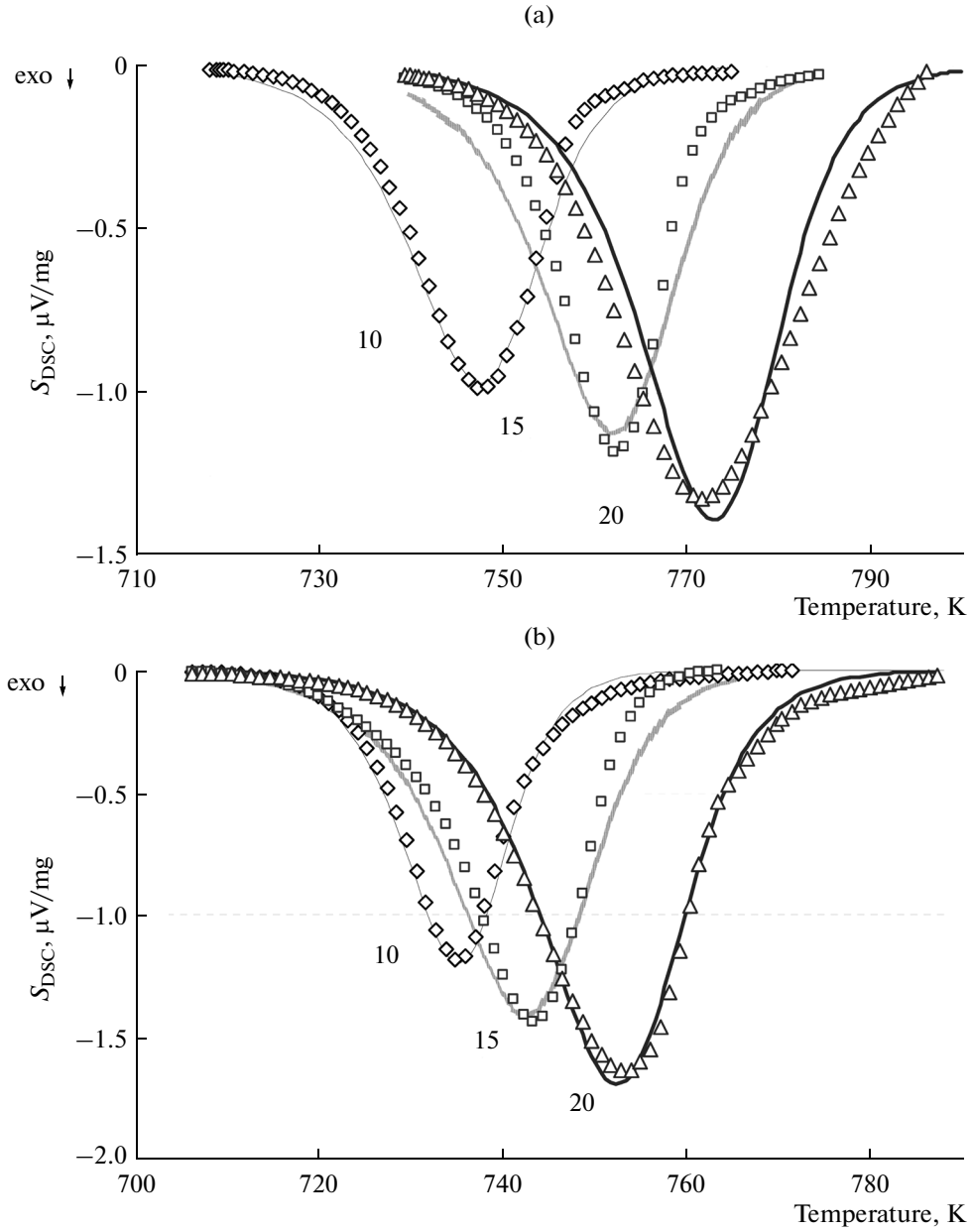

Fig. 3. Experimental data (open data points) and crystallization peaks calculated in the MSE model (solid lines), with parameters evaluated by data processing (Table 3), at different heating rates (β, K/min, is indicated at the curves) for the glasses with the compositions (a) $(TeO_2)_{0.75}(MoO_3)_{0.25}$, (b) $(TeO_2)_{0.65}(MoO_3)_{0.35}$, (c) $(TeO_2)_{0.60}(MoO_3)_{0.40}$, (d) $(TeO_2)_{0.55}(MoO_3)_{0.45}$, and (e) $(TeO_2)_{0.45}(MoO_3)_{0.55}$.

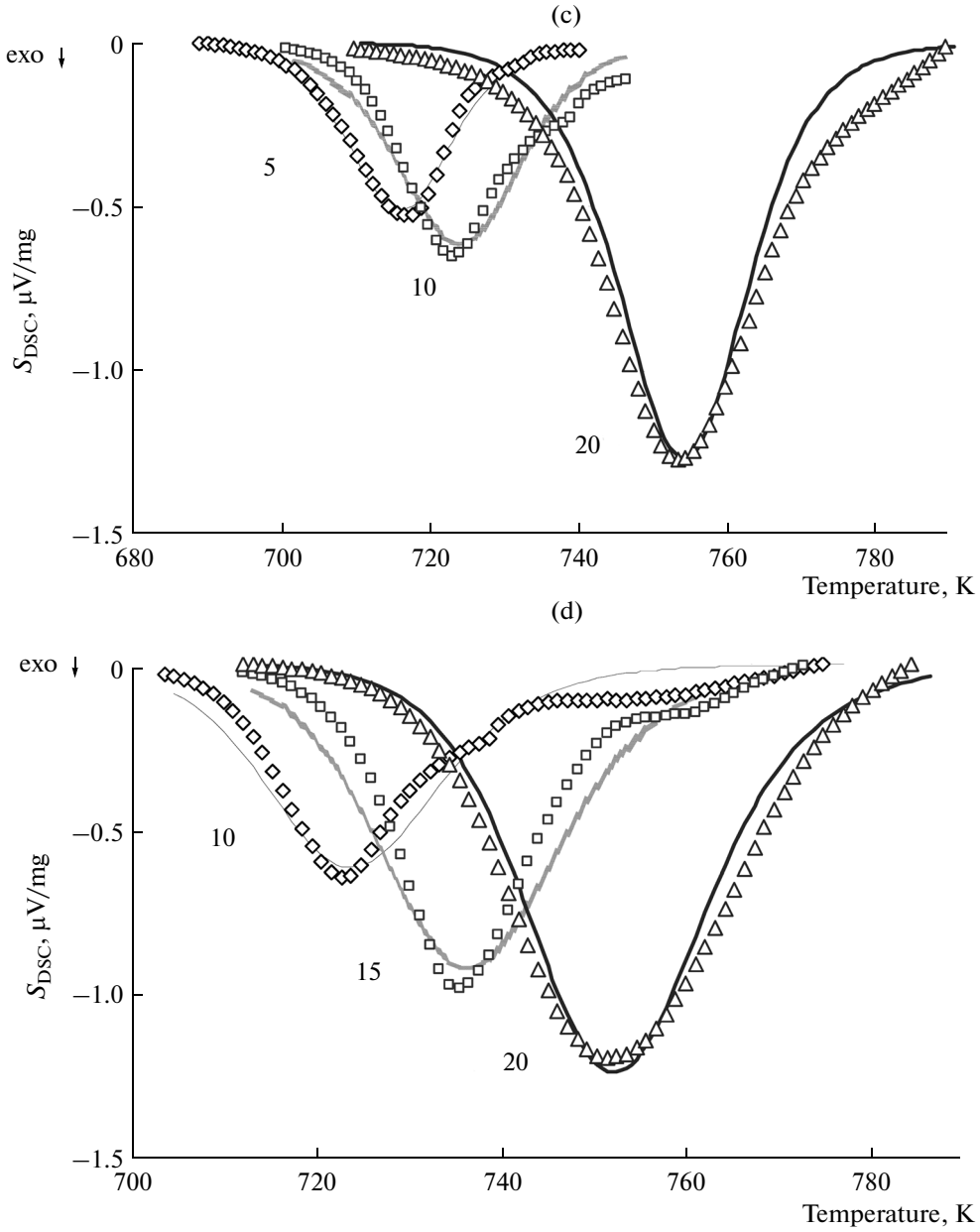

Fig. 3. (Contd.)

peak in Fig. 3a is influenced to different extents by the additional peak of the TeO_2 phase, instead of MoO_3. Finally, Fig. 3b demonstrates that, in the case of the glass close in composition to the Te_2MoO_7 compound, the slight excess of MoO_3 has no significant effect on the main crystallization peak of Te_2MoO_7.

The present DSC data on the crystallization kinetics of the $(TeO_2)_{1-x}(MoO_3)_x$ tellurite–molybdate glasses demonstrate that, in the composition range $x = 0.25–0.55$, a major crystallizing phase is Te_2MoO_7. The parameters obtained by a model analysis of crystallization peaks (Table 3) on the whole reflect the sequential and concurrent crystallization of the above phases, in addition to the major phase.

Figure 4 shows the crystallization parameters E_a, s, n, and p and the np product of the exponents as functions of glass composition, together with regression relations. The $\alpha(t, T)$ temperature–time diagrams (6) calculated from these parameters provide a basis for predicting heat treatment temperatures and durations capable of minimizing glass crystallization and its contribution to the optical losses in the glasses.

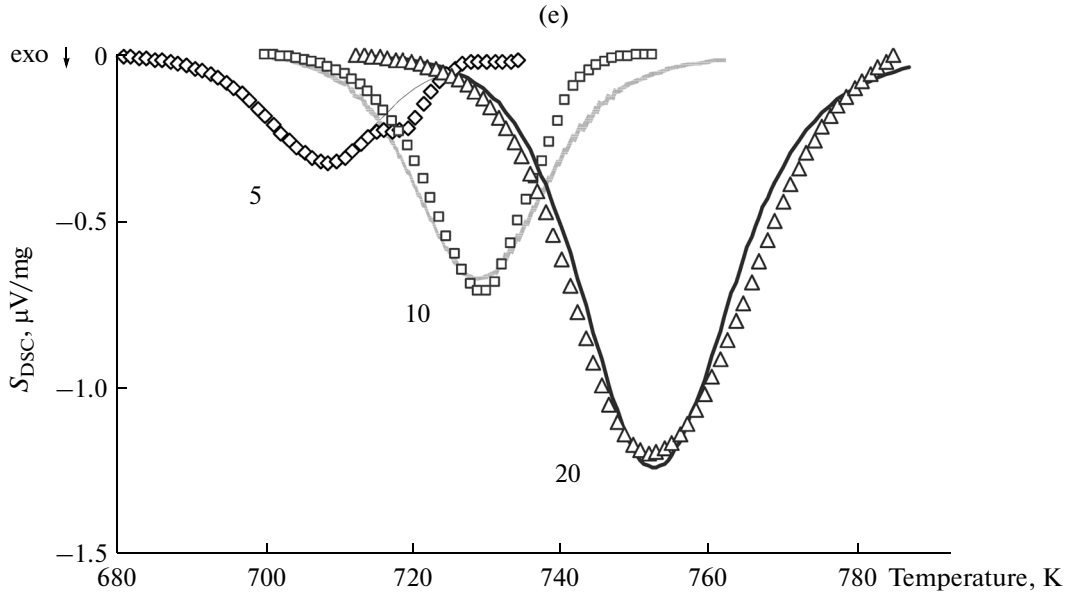

Fig. 3. (Contd.)

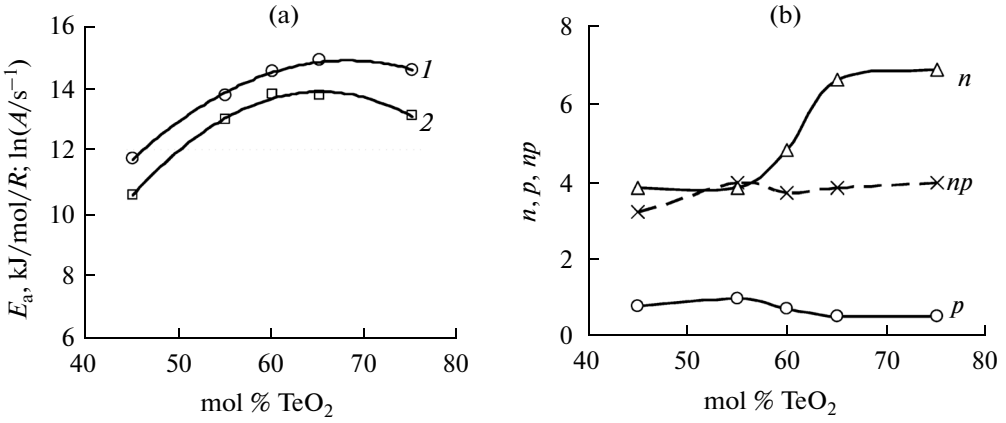

Fig. 4. Model kinetic parameters of glass crystallization (data points) and their dependences on glass composition (lines): (a) activation energy (E_a), pre-exponential factor (A), and their regression equations: (*1*) E_a, kJ/mol/$R = -0.0059z^2 + 0.8091z - 12.672$, (*2*) $\ln(A/s^{-1}) = -0.0082z^2 + 1.0627z - 20.7544$, where z is the mole percent of TeO_2; (b) n and p exponents, np product, and corresponding smoothed lines.

CONCLUSIONS

A new technique has been proposed for analysis of glass crystallization peaks which takes into account that DSC measurements are made under nonisothermal conditions. Its effectiveness has been confirmed by test data on GeS_2 glass crystallization kinetics. It relies on a modified semiempirical form of the Kolmogorov–Johnson–Mehl crystallization theory.

Analysis of DSC curves for five $(TeO_2)_{1-x}(MoO_3)_x$ ($x = 0.25$–0.55) glass samples by the proposed technique allowed us to find general parametric crystallization relationships for calculating the degree of crystallization as a function of temperature and time under various glass heat treatment conditions, in particular with prediction possibilities for previously unexplored compositions.

According to the phase diagram reported by Petrini and Bart [14], the distinctive features of glass crystallization, manifest as additional peaks, are due to the crystallization of the Te_2MoO_7 phase and the TeO_2 or MoO_3 end-member as an additional phase, depending on glass composition.

Note also that no technique has been proposed to date for processing DSC data on multiphase crystallization kinetics in binary or multicomponent glasses. From the viewpoint of the approach in question, the development of such a technique is facilitated by the presence of an explicit $\alpha(t, T)$ functional dependence.

ACKNOWLEDGMENTS

This work was supported by the Russian Foundation for Basic Research, grant no. 14-03-31376 mol_a.

REFERENCES

1. Sibirkin, A.A., Zamyatin, O.A., Torokhova, E.V., Churbanov, M.F., Suchkov, A.I., and Moiseev, A.N., Coprecipitation of tellurium and molybdenum oxides from aqueous solutions, *Inorg. Mater.*, 2011, vol. 47, no. 10, pp. 1214–1217.
2. Churbanov, M.F., Sibirkin, A.A., and Zamyatin, O.A., RF Patent 2484026, *Byull. Izobret.*, 2013, no. 16.
3. Sibirkin, A.A., Zamyatin, O.A., Torokhova, E.V., and Suchkov, A.I., Coprecipitation of tellurium(IV) and molybdenum(VI) hydroxides from aqueous hydrochloric acid solutions, *Vestn. Nizhegorodsk. Univ. im. N.I. Lobachevskogo*, 2008, no. 6, pp. 88–93.
4. Stkuja, T., Moshida, N., and Ogawa, S., Structural study of MO_3–TeO_2 glasses, *J. Non-Cryst. Solids*, 1995, vol. 185, pp. 135–144.
5. Hohne, G.W.H., Hemminger, W.F., and Flammersheim, H.J., *Differential Scanning Calorimetry*, Berlin: Springer, 2003, 2nd ed.
6. Šesták, J., *Thermophysical Properties of Solids: Their Measurements and Theoretical Thermal Analysis*, Prague: Academia, 1984.
7. Malek, J., Zmrhalova, Z., Bartak, J., and Honcova, P., A novel method to study crystallization of glasses, *Thermochim. Acta*, 2010, vol. 511, pp. 67–73.
8. Malek, J. and Klikorka, J., Crystallization kinetics of glassy GeS_2, *J. Therm. Anal.*, 1987, vol. 32, pp. 1883–1893.
9. Prigogine, I. and Kondepudi, D., *Modern Thermodynamics: From Heat Engines to Dissipative Structures*, Chichester: Wiley, 1998. Translated under the title *Sovremennaya termodinamika. Ot teplovykh dvigatelei do dissipativnykh struktur*, Moscow: Mir, 2002, p. 461.
10. Borchard, H.J. and Daniels, F., The application of differential thermal analysis to the study of reaction kinetics, *J. Am. Chem. Soc.*, 1957, vol. 79, pp. 41–46.
11. Young, D.A., *Decomposition of Solids*, Oxford: Pergamon, 1966. Translated under the title *Kinetika razlozheniya tverdykh veshchestv*, Moscow: Mir, 1969, p. 263.
12. Sestaik, J. and Berggren, G., The study of the kinetics of mechanism of solid-state reactions at increasing temperature, *Thermochim. Acta*, 1971, vol. 3, pp. 1–12.
13. Sibirkin, A.A., Zamyatin, O.A., Churbanov, M.F., Moiseev, A.N., and Pimenov, V.G., Impurity composition of molybdate–tellurite glasses prepared from mixtures precipitated from hydrochloric acid solutions of tellurium and molybdenum compounds by ammonia, *Inorg. Mater.*, 2013, vol. 49, no. 2, pp. 219–222.
14. Petrini, G. and Bart, J.C.J., Das Phasendiagramm des Systems TeO_2–MoO_3, *Z. Anorg. Allg. Chem.*, 1981, vol. 474, pp. 229–232.

Translated by O. Tsarev